IEEE Access
Multidisciplinary | Rapid Review | Open Access Journal

Received 8 January 2023, accepted 23 January 2023, date of publication 30 January 2023, date of current version 2 February 2023.

Digital Object Identifier 10.1109/ACCESS.2023.3240443

RESEARCH ARTICLE

Multiple Types of Cancer Classification Using CT/MRI Images Based on Learning Without Forgetting Powered Deep Learning Models

MALLIGA SUBRAMANIAN[1], JAEHYUK CHO[2], VEERAPPAMPALAYAM EASWARAMOORTHY SATHISHKUMAR[2], AND OBULI SAI NAREN[1]

[1]Department of Computer Science and Engineering, Kongu Engineering College, Erode 638060, India
[2]Department of Software Engineering, Jeonbuk National University, Jeonju-si, Jeollabuk-do 54896, South Korea

Corresponding author: Jaehyuk Cho (chojh@jbnu.ac.kr)

This work was supported in part by the Korea Environmental Industry and Technology Institute (KEITI) Grant through the Korean Government (Ministry of the Environment), the Development of the IoT-Based Technology for Collecting and Managing Big Data on Environmental Hazards and Health Effects, under Project RE202101551; in part by the Institute of Information and Communications Technology Planning and Evaluation (IITP) Grant through the Korean Government, Ministry of Science and ICT (MIST), Implementation of 5G-Based Smart Sensor Verification Platform, under Grant 2019-0-00135; and in part by IITP through the Korea Government, MSIT, Building a Digital Open Laboratory as Open Innovation Platform, under Grant 2021-0-00546.

ABSTRACT Cancer is the second biggest cause of death worldwide, accounting for one of every six deaths. On the other hand, early detection of the disease significantly improves the chances of survival. The use of Artificial Intelligence (AI) to automate cancer detection might allow us to evaluate more cases in less time. In this research, AI-based deep learning models are proposed to classify the images of eight kinds of cancer, such as lung, brain, breast, and cervical cancer. This work evaluates the deep learning models, namely Convolutional Neural Networks (CNN), against classifying images with cancer traits. Pre-trained CNN variants such as MobileNet, VGGNet, and DenseNet are employed to transfer the knowledge they learned with the ImageNet dataset to detect different kinds of cancer cells. We use Bayesian Optimization to find the suitable values for the hyperparameters. However, transfer learning could make it so that models can no longer classify the datasets they were initially trained. So, we use Learning without Forgetting (LwF), which trains the network using only new task data while keeping the network's original abilities. The results of the experiments show that the proposed models based on transfer learning are more accurate than the current state-of-the-art techniques. We also show that LwF can better classify both new datasets and datasets that have been trained before.

INDEX TERMS Cancer, convolutional neural network (CNN), pretrained models, Bayesian optimization, transfer learning, learning without forgetting, VGG16, VGG19, DenseNet, mobile net.

I. INTRODUCTION

The term ''cancer'' describes a situation in which the body's normal cells develop abnormally due to uncontrolled mutations. Upon creation, these cells divide erratically and disseminate throughout the organs. If left untreated, most cancers have the potential to kill us. The leading cause of death worldwide is cancer, followed by cardiovascular diseases. Any part of the body can develop cancer cells, but the most common sites are the lungs, breasts, brain, colon, rectum, liver, stomach, skin, and prostate. A myriad of factors, including behavioral qualities like a high BMI, cigarette and alcohol consumption, physical carcinogens like UV rays and radiation, etc causes cancer. In addition, discomfort, tiredness, persistent cough, nausea, breathing problems, bruising, bleeding, weight loss, muscle pain, and other cancer symptoms are prevalent. Hence, diagnosing cancer at its earliest stages often provides the best chance for a cure. Four modalities are

The associate editor coordinating the review of this manuscript and approving it for publication was Wentao Fan.

available to clinicians who diagnose, stage, and treat human cancer: physical examination, laboratory tests, imaging techniques, and biopsy. Of these, imaging techniques such as Computed Tomography (CT), Magnetic Resonance İmaging (MRI), etc, are capable of 3D detection of cancer anywhere in the human body. Figure 1. shows a few types of imaging techniques.

Among various techniques to detect the presence of cancer cells, CT and MRI provide a wealth of information on tumor location, size, morphology, and structural changes in the surrounding tissues. Physicians and health practitioners use these images to detect and locate cancer cells in the human body. But, visual inspection of MRI /CT scans sometimes results in false positive diagnoses. Consequently, improved computer-assisted diagnosis techniques are essential for reliably confirming the presence of cancer cells.

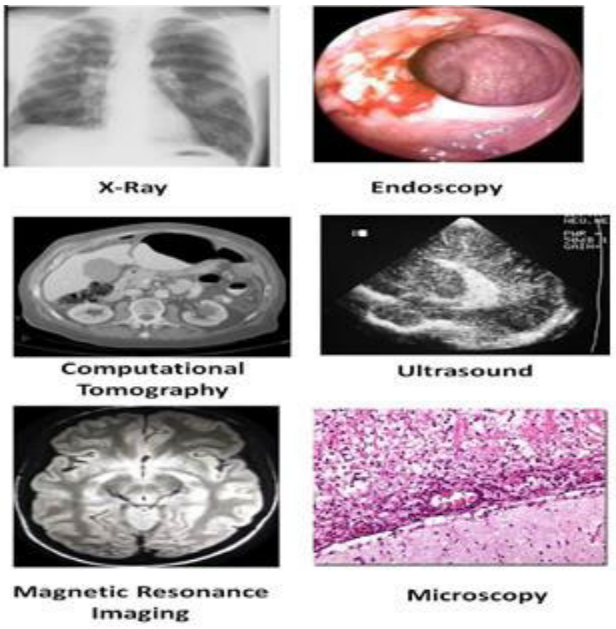

FIGURE 1. Various imaging techniques.

As the use of Artificial Intelligence (AI) in health care continues to grow, researchers are finding new ways to use deep learning models. Deep learning has been very important for diagnosing, making decisions about, and treating chronic diseases, especially in cancer research. A study [1] found that deep learning models can find and diagnose cancer as well as or better than pathologists by looking at scans of tissue. This study suggests that pathologists use more prescreening technology to make diagnoses faster. Deep learning models can not only find cancer earlier, but they can also improve detection accuracy. Deep learning based computer vision algorithms specializing in image recognition have been applied to medical imaging techniques such as CT and MRI scans [2], [3], [4], [5]. Several attempts have been made to extract image information, including spatial correlations, via medical imaging-based deep learning algorithms. Particularly in the extraction of features, CNN's performance was exceptional. CNNs excelled at numerous computer vision tasks [4], [6]. CNNs have become the primary deep learning method for medical image categorization in recent years due to their self-learning capabilities. Numerous CNN-based neural network models have been advocated for identifying various diseases [6]. The primary objective of this study is to develop effective strategies for using CNN to detect various forms of cancer. For this research, we have collected CT/MRI images of eight types of cancer, namely Acute Lymphoblastic Leukemia (ALL), Brain Cancer, Breast Cancer, Cervical Cancer, Kidney Cancer, Lung, and Colon Cancer, Lymphoma, and Oral Cancer. Through this work, we intend to address the following research questions:

RQ1: How can models that have been pre-trained be customized to classify the images in a new dataset?

We have finetuned the pre-trained CNN models and then compared how well they worked for a new dataset with images of four types of cancer: acute lymphoblastic leukemia, cervical, kidney, and breast cancer.

RQ2: How effective can fine-tuning the hyperparameters of different CNN models be?

Given the importance of these values in determining how well a model performs, we used Bayesian optimization to select the best values for hyperparameters.

RQ3: Can models use what they've learned from one task or dataset to do something new and excel in both original and new datasets?

To look into this problem, we used a set of CT/MRI images of four other types of cancer: lymphoma, lung and colon, brain tumor, and oral cancer.

In this study, we develop a set of models using pre-trained CNN architectures to automatically detect and characterize different types of cancer from CT/MRI images, which have been acquired from diverse sources such as Kaggle, etc. To fine-tune pre-trained models for repurposing, we have retrained a few top feature extraction layers and replaced the classification layer at the top. In order to determine the ideal values for the hyperparameters used to train various CNN architectures, this work also uses Bayesian optimization.

The following are the substantial contributions to this work:

i. Acquired CT/MRI images for different types of cancer from different sources and preprocessed the images

ii. Investigated the performance of CNN variants using transfer learning, fine-tuning, and exhaustive simulations.

iii. Explored Bayesian optimization to hyperparameter optimization

iv. Transferred the knowledge acquired by the proposed models to a standard, challenging dataset comprising CT/MRI scans of another four types of cancer.

We analyze the performance of five CNN architectures using transfer learning over the CT/MRI image dataset. In addition, Learning without Forgetting (LwF) is investigated as a solution for multitask learning. To our knowledge, no previous work has focused on transfer learning with LwF

and Bayesian Optimization for categorizing CT/MRI images of multiple cancer cells.

The remainder of the paper is structured as follows: Section II summarizes recent cancer classification efforts with CNNs based on deep learning. Section III describes the materials and procedures utilized in this work. In Section IV, the recommended models are explained. The experimental findings and performance of the proposed models are shown in Section V. In this section, the rationale for employing LwF is also discussed. Section VI finally concludes this work.

II. RELATED WORKS

Several traditional approaches for detecting and classifying tumors are simple and complicated, requiring more time and labor around the clock. Recently, deep learning models have been used to conduct cancer classification. İn this section, we summarize the recent attempts on detecting/ classifying a variety of cancer using deep learning models.

Deep learning networks such as VGG-16 and ResNet-50 were utilized by Rezayi et. al. [7] for detecting acute lymphoblastic leukemia. In addition, the authors presented a CNN with 10 convolutional layers and six common machine learning algorithms for dividing leukemia into two groups. The authors compared various ML and CNN models in detecting this condition and concluded that CNN outperformed ML models. Gunasekara et. al. [8] proposed a three-fold deep learning architecture with classifiers implemented with a deep CNN at the first level, and at the second level, a region-based CNN (R-CNN) to locate the tumor regions of interest. The ChanVese segmentation algorithm is used to contour the concentrated tumor boundaries for segmentation in the final stage. The average dice score for this model is 0.92.

To further understand how textural, morphological, and graph properties affect categorization classification accuracy, Reshma et. al. [9] conducted a series of studies. An improved Genetic Algorithm and a weighted feature selection method in conjunction with CNN have been proposed to detect breast cancer. Zhao et al. [10] found that adding manual features and a vote system can produce outstanding accuracy in cervical cell categorization even with little amounts of labeled data. A small number of images are annotated using a clarity function, and a voting mechanism is used to balance the training data for the algorithm. The proposed method in this research [10] has a 91.94% accuracy rate with only a little amount of labeled data. Pederson et. al. explored the efficacy of CNNs to facilitate the distinction of oncocytoma from renal cell carcinoma [11]. The authors suggested a revised version of the ResNet50V2 as a solution. A majority vote of individual image classifications determined a renal tumor's benign or malignant nature, which was set at 51%. By analyzing the histological images of lung and colon tissues, Masud et. al. [12] developed a categorization framework that enabled them to differentiate between five distinct lung and colon tissues, two benign and three malignant. According to the findings, this framework has a maximum accuracy of 96.33% in determining whether or not tissues contain cancer.

Khan et. al. [13] suggested a CNN-based hierarchical deep learning-based brain tumor classifier and used it to classify the input into the following four categories: glioma, meningioma, pituitary, and non-tumor. This model achieved an accuracy of 92.13%, making it superior to the various approaches currently used to detect and segment brain tumors. Alanazi et al. [14] came up with the idea of using a CNN to improve the accuracy of the automatic detection of breast cancer. The analysis of hostile ductal carcinoma tissue zones in whole-slide images was done. In addition, the authors explored models that use a variety of CNN architectures to automatically diagnose breast cancer. They compared the findings of these models to those produced by machine learning techniques. To segment the colon and polyps from CT images, a deep CNN-based residual network technique provided by Akilandeswari et al. [15] has been adopted over the 2D CT images. The residual stack block and the short skip nuance have been implemented in the hidden layers to preserve the spatial data. Here, ResNet-enabled CNN is used for thorough segmentation of colon cancer region.

İn an attempt, a classification and detection model was developed by Warin et. al. [16] utilizing DenseNet121 and a faster R-CNN. According to the findings of these authors, the above algorithms were proven to have adequate potential for identifying malignant tumors in images. Finally, Tufail et. al. [17] described recent works where deep learning has been used to determine the most effective models for cancer prediction tasks. This work focused on analyzing the effect that deep learning systems have on histopathology images, presented a synopsis of state-of-the-art deep learning approaches, and provided future researchers with guidance on how to improve upon the methods that are now in use.

From the review of the existing research attempts, we see that the performance of the contemporary models, such as ResNet, MobileNet, DenseNet etc is appreciable compared to traditional models such as VGGNet, AlexNet etc. We have already enumerated the research questions in Section I. These research questions have been framed from the following points. From the literature study, we find that pretrained CNN models with transfer learning provide a number of advantages over traditional CNN models, including faster performance, fewer data requirements, and reduced training time. Hyperparameters govern the learning process, and as a result, these parameters' values directly impact other model parameters like weights and biases, which in turn affects how well a model performs. While using transfer learning, the models may forget their previous knowledge when retrained on a new task set. Since, we want to retain previous knowledge along with the new task set, we use LwF.

To summarize, the attempts to detect cancer tissue presence from CT/MRI images focused mostly on one or two types of cancer. In the present work, we try to detect multiple kinds of cancer. Recent publications suggest that deep learning models are used more frequently for cancer detection in CT/MRI and

other imaging modalities. However, the use of deep learning architectures still has space for improvement, particularly in terms of training time and hyperparameter adjustment. Our goal is to build a few classification models that can classify different types of cancer cells using a combination of neural network techniques such as deep learning, transfer learning, and hyperparameter tuning. Further, we use LwF to retain the original network capabilities while training the models on new cancer datasets.

III. MATERIALS AND METHODS

A. IMAGE COLLECTION

The image collection is the process of gathering images from different sources. The present study focuses on detecting a variety of cancer namely ALL, Brain Cancer, Breast Cancer, Cervical Cancer, Kidney Cancer, Lung and Colon Cancer, Lymphoma, and Oral Cancer. CT/MRI images for the various body parts (tissues) are collected and compiled from Kaggle containing the categories ALL [18], Breast Cancer [19], Cervical Cancer [20], Kidney Cancer [21], Lung and Colon Cancer [22], Lymphoma [23] and Oral Cancer [24]. In addition, an open-source Brain tumor Image Database [25] containing different MRI images with different pathological conditions have been generated. Each type of cancer has a few categories as listed in Table 1.

TABLE 1. Different types of cancer and their categories.

Main Cancer Types	Number of Subclasses	Subclasses
ALL	4	Benign, Pre, Pro, Early
Brain Cancer	3	Glioma Meningioma Pituitary Tumor
Breast Cancer	2	Benign, Malignant
Cervical Cancer	5	Dyskeratotic Koilocytotic Metaplastic Parabasal Superficial-Intermediate
Kidney Cancer	2	Normal, Tumor
Lung and Colon Cancer	5	Lung Benign Tissue Lung Adenocarcinoma Lung Squamous Cell Carcinoma, Colon Adenocarcinoma Colon Benign Tissue
Lymphoma	3	Chronic Lymphocytic Leukemia Follicular Lymphoma Mantle Cell Lymphoma
Oral Cancer	2	Normal Oral Squamous Cell Carcinoma

B. IMAGE PREPROCESSING AND AUGMENTATION

Since the images have been acquired from different sources, they differ in number, format, and size. Hence, the datasets must be preprocessed before being used to input any model. As the images from the dataset are of different formats such as JPEG, JPG, PNG, BMP, NII, and TIF, they have been converted to JPG format uniformly. As like formats, the images in the dataset differ in dimensions. So, they have all been resized to 224*224 (common for all models) and labeled according to their classes.

1) IMAGE AUGMENTATION

There are a few challenges when we use deep learning models for image classification. The more information the deep learning models have, the more features they will be able to learn. For deep learning models to learn more features, enormous volumes of data are required. Having this much information is only sometimes simple, though. Additionally, sometimes, we may have a lot of data on a certain subject, but it is frequently unlabeled, which prevents us from using it to train learning algorithms. Since we don't have a balanced image dataset for each type of cancer, we used image augmentation, which is a way to make new images from the ones in the training set. Table 2 lists the number of images in each category. Rotation, shifting, cropping, blurring, scaling, flipping horizontal and vertical, and padding are examples of image augmentation methods to minimize the model's overfitting. After augmentation, the dataset consists of around 130000 images, with 5000 images in each category of all types of cancer. The number of images in each class after augmentation is shown in Figure 2.

Hence, using augmentation, we have constructed a new dataset and uploaded it as a public dataset on Kaggle under the name "Multi Cancer Dataset" [26]. Next, the deep learning model we train should be tested and evaluated against the performance. For this, the dataset is split into 70:15:15 ratio for training, validation, and testing.

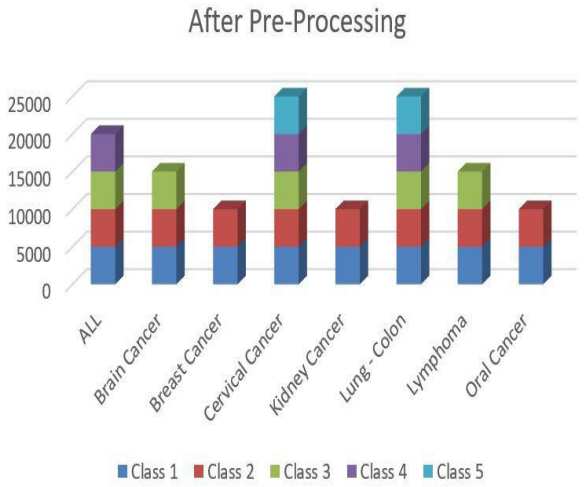

FIGURE 2. Number of Images after augmentation.

C. METHODS AND MODELS

The development of several CNN architectures for image recognition applications has resulted in their effective

application to various difficult visual imagery challenges. In this study, the ability of five different CNN architectures, namely VGG16, VGG19, DenseNet201, MobileNetV3 (Small) and MobileNetV3 (Large) to classify the types of cancer from CT/ MRI images has been evaluated. The basic CNN is explained below.

TABLE 2. Number of actual images in the dataset.

Types of cancer	Subclasses	Number of images	
		Category-wise	Total
Lymphoma	Chronic Lymphocytic Leukemia	113	374
	Follicular Lymphoma	139	
	Mantle Cell Lymphoma	122	
ALL	Benign	504	3256
	Early	985	
	Pre	963	
	Pro	804	
Breast Cancer	Benign	2479	7783
	Malignant	5304	
Lung and Colon Cancer	Lung Benign Tissue	5000	25000
	Lung Adenocarcinoma	5000	
	Lung Squamous Cell Carcinoma	5000	
	Colon Adenocarcinoma	5000	
	Colon Benign Tissue	5000	
Kidney Cancer	Normal	2283	7360
	Tumor	5077	
Oral Cancer	Normal	2494	5192
	Oral Squamous Cell Carcinoma	2698	
Cervical Cancer	Dyskeratotic	223	966
	Koilocytotic	238	
	Metaplastic	271	
	Parabasal	108	
	Superficial-Intermediate	126	
Brain Cancer	Glioma	1426	3064
	Meningioma	708	
	Pituitary Tumor	930	

For image categorization, CNN is a popular deep learning technology. It's also useful for modeling applications that require a lot of data and is positioned at the top of its field [27], [28]. A gradient-based strategy was used by Lecun et. al. [29] to solve the problem of categorizing hand-written digits using CNNs. With this success came the recognition of language and activities, and now it is used in a wide range of fields, including object tracking and identification. A CNN can be broken into two basic building blocks: a feature extractor and a classifier. The block for feature extraction consists of convolutional and pooling layers. The classification layer is fully connected and flattened. The filters comprising a convolutional layer indicate lower-dimensional input data characteristics. To construct feature maps, the filters convolute the entire input image. The pooling layers are then employed to lower the dimensionality of the feature maps, and the feature maps are subsequently downsampled. The last convolution layer flattens the feature map. Finally, two or three hidden layers and an output layer that uses a classifier to differentiate between two or more classes are at the classifier part. Despite their primary application in image classification, CNNs are increasingly used for feature extraction and classification in many image processing applications. Figure 3 depicts a typical CNN.

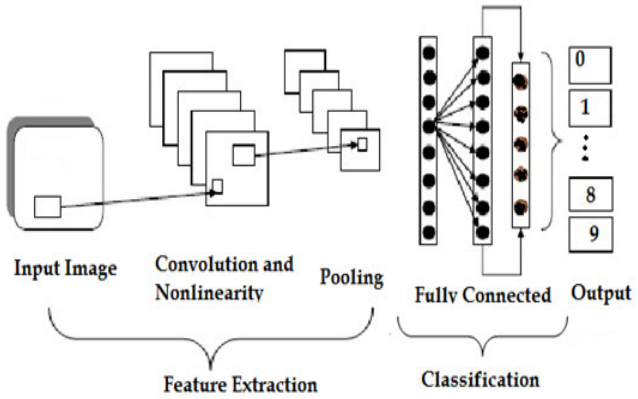

FIGURE 3. Architecture of CNN (Adapted from: https://link.springer.com/article/10.1007/s00521-022-07246-w).

The first few layers of a CNN are usually responsible for finding basic things like horizontal, vertical, and diagonal edges, among other things. The results of these layers are sent to the layers in the middle, whose job is to pull out more complex features like corners and edges. As we go deeper into the network, the layers start recognizing higher-level things like objects, faces, and other things. Several CNN variants have been developed and effectively applied to challenging visual tasks for image recognition applications. In this study, we choose to develop the proposed models using pre-trained models such as VGG16, VGG19, DenseNet201, MobileNetV3 (small), and MobileNetV3 (large) which are the variants of CNN.

D. TRANSFER LEARNING WITH FINETUNING

Transfer learning entails transferring the information of a model learned on a big dataset to a smaller dataset. Typically, the pre-trained models are trained on enormous datasets that serve as a typical benchmark for computer vision tasks, such as ImageNet [30]. Canziani et. al. [31] investigated the efficacy of pre-trained computer vision models using the ImageNet database. The weights derived from the models are reusable for various computer vision tasks [32]. The justification for employing pre-trained CNN models is that the earliest convolutional layers of the models extract broad, low-level features that are relevant across images, such as edges, patterns, and gradients, while the subsequent layers detect unique image properties. In the present study, we categorize the dataset under consideration using the models such as VGG16, VGG19, DenseNet201, MobileNetV3 (small) and MobileNetV3 (large). Because the early layers can acquire general features, we have reused the weights of these layers, but, we retrain a few top layers of the feature extraction (convolution base) component. This is done so that the models can learn the characteristics unique to the datasets. In the

classifier part, we added a layer with the number of labels corresponding to the number of unique classes in the dataset. Then, the output of the convolution base is passed into this classifier.

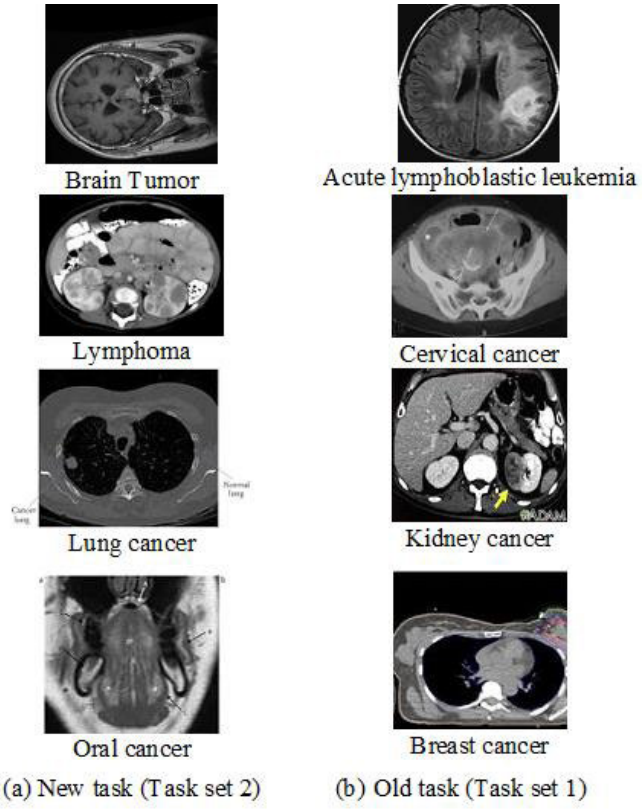

FIGURE 4. CT/MRI Images of older and new tasks.

E. LEARNING WITHOUT FORGETTING(LwF)

Even while pre-trained CNNs use transfer learning, they may forget what they had previously learned when transferring that knowledge to a new task. Transfer learning typically disregards the model's performance on previous tasks. For example, a CNN that has been pre-trained to identify items such as flowers, animals, etc. may not perform well when used to classify different animal types. Because the shared parameters do not adequately reflect what distinguishes the new task, feature extraction typically fails when applied to the new task. If we fine-tune, it may decrease performance for previously learnt tasks, as the shared parameters will change without providing a new direction for the task-specific prediction parameters. To overcome this issue, Learning without Forgetting (LwF) [33], a multitasking approach, has been developed; it works effectively on new tasks while maintaining the same performance on previous ones. While learning new tasks, we frequently use the knowledge we gained from the related tasks. This is termed as multitasking learning (MTL). By employing the domain knowledge in the training task of related tasks as an inductive bias, the MTL approach to inductive transfer enhances generalization. Formally, MTL will assist in improving the learning of a particular model by using the knowledge contained in all of the 'n' tasks if there are 'n' tasks where these 'n' tasks or a subset of them are related to each other but not exactly identical. When only data from new tasks are available, LwF aims to train a network on effectively performing both old and new tasks. With this method, results from the previous network are retained, and samples from the new task are used to enhance the accuracy of the new task. However, this method does not require the previous task's images and labels. In this attempt, we employed CT/MRI images depicting the symptoms of four types of cancer cells, including lymphoma, lung/colon, brain tumor, and oral cancer, how LwF determines what they are. Figure 4 shows a few CT images that bear both old (Task set 1) and new tasks (Task set 2).

The rationale behind splitting the dataset into two task sets is to evaluate the models' performance with and without LwF. Task set 2 has images of different oral, leukemia, lung/colon, and brain cancer subclasses. The images of breast cancer, acute lymphoblastic leukemia, kidney, and cervical cancer are under task set 1. Since the survivors of the task set 1 types of cancer are at risk of falling into the types of cancer in task set 2 [34], [35], [36], we split as above.

F. BAYESIAN OPTIMIZATION FOR HYPERPARAMETER TUNING

The number of hidden units, dropout, activation function, weight initialization, and other hyperparameters establish a neural network's structure, whereas learning rate, batch size, epochs, etc. Tuning hyperparameters minimizes a loss function and improves results. Unlike Grid and Random search methods, Bayesian optimization employs previous iterations of the algorithm. This facilitates Bayesian optimization to choose the optimal combination of the hyperparameters for model evaluation [37], [38]. Due to the volume of data involved and the complexity of computations necessary, training deep learning models can be time-consuming. When dealing with issues of this kind, employing Bayesian optimization can significantly assist problem-solving. So, we employ Bayesian optimization in conjunction with previously trained models to enhance performance. Fig. 5 illustrates the proposed flow of the research work.

IV. DETAILS OF EXPERIMENTS

We designed experiments to evaluate the performance of the fine-tuned models using transfer learning and LwF. In the following section, we present the details of the same.

A. EXPERIMENTAL PLATFORM

Graphical Processing Units (GPU) were employed to run the proposed models due to their high power consumption and requirement for high-performance hardware. Table 3 shows the employed hardware and software configurations. We imported the Keras model architectures and instantiated them with the ImageNet dataset TABLE 3.

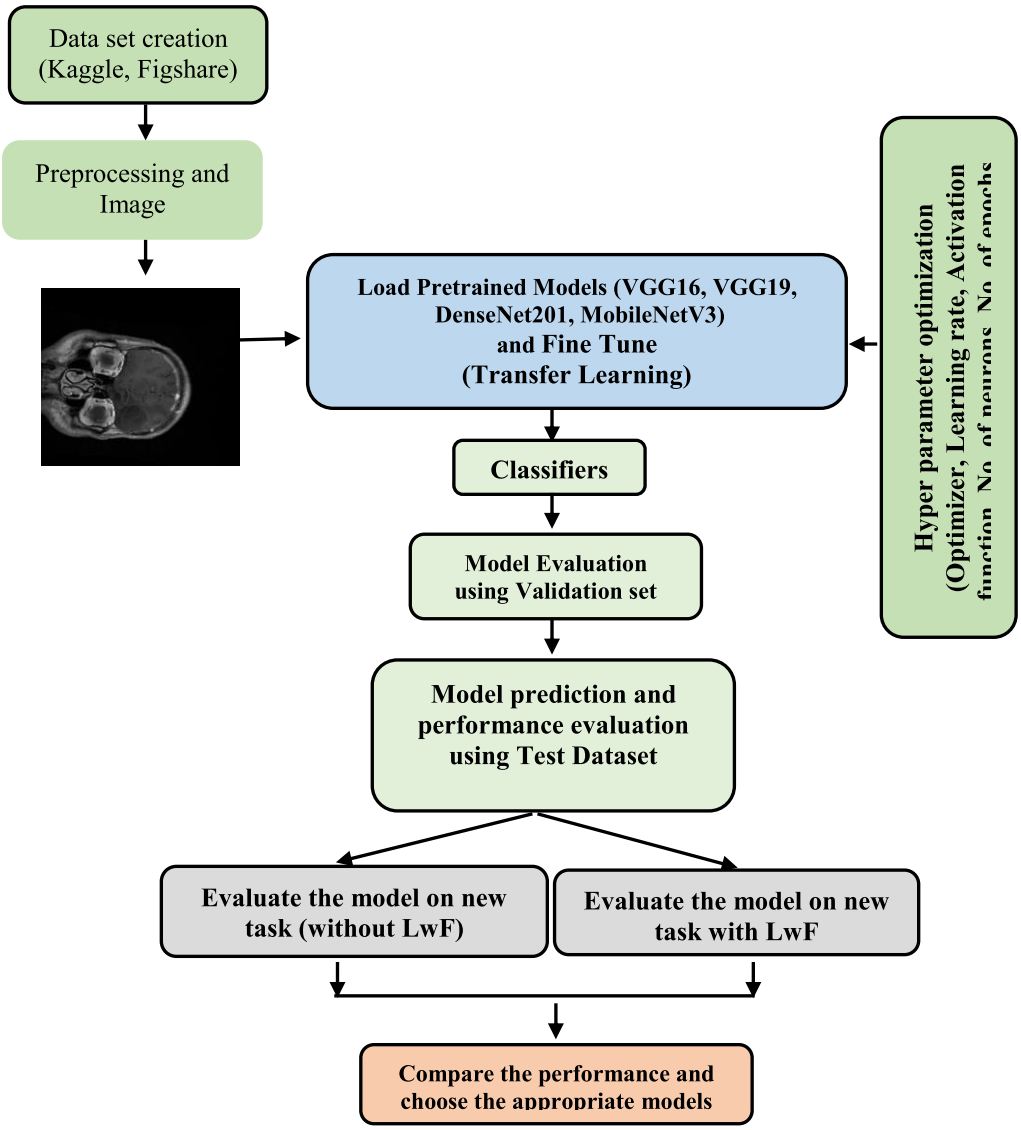

FIGURE 5. Proposed workflow.

TABLE 3. Experimental platform.

Parameters	Details
GPU	DELL 740 with EMC
RAM	128 GB
GPU RAM	32 GB
DISK	4TB
OS	Ubuntu
Language	Python
IDE	Jupyter on Google Co-laboratory

B. TUNING OF HYPERPARAMETERS

Hyperparameters are crucial in determining training parameters and influencing model output when utilizing deep learning algorithms. This study applies Bayesian optimization to determine the optimal hyperparameter values while assuring high accuracy. Using Bayes' theorem, this method can determine an objective function's lowest or maximum value. Among the fine-tuned hyperparameters are optimizers, learning rate, activation function, number of epochs, batch size, and the number of neurons. The Bayesian optimization procedure has been executed twenty times. The number of epochs for each round of Bayesian optimization is set at 150. At each stage, we kept track of our performance and losses. The hyperparameters we deal with and their respective search spaces are shown in Table 4. Table 4 also presents the tuned values of hyperparameters for different models. Figure 5 shows the overall steps involved in the proposed workflow.

C. METRICS FOR EVALUATION

We evaluated the performance of each model against each of the thirteen classes belonging to four types of cancer using accuracy, precision, recall, and F1-score. To find the values of

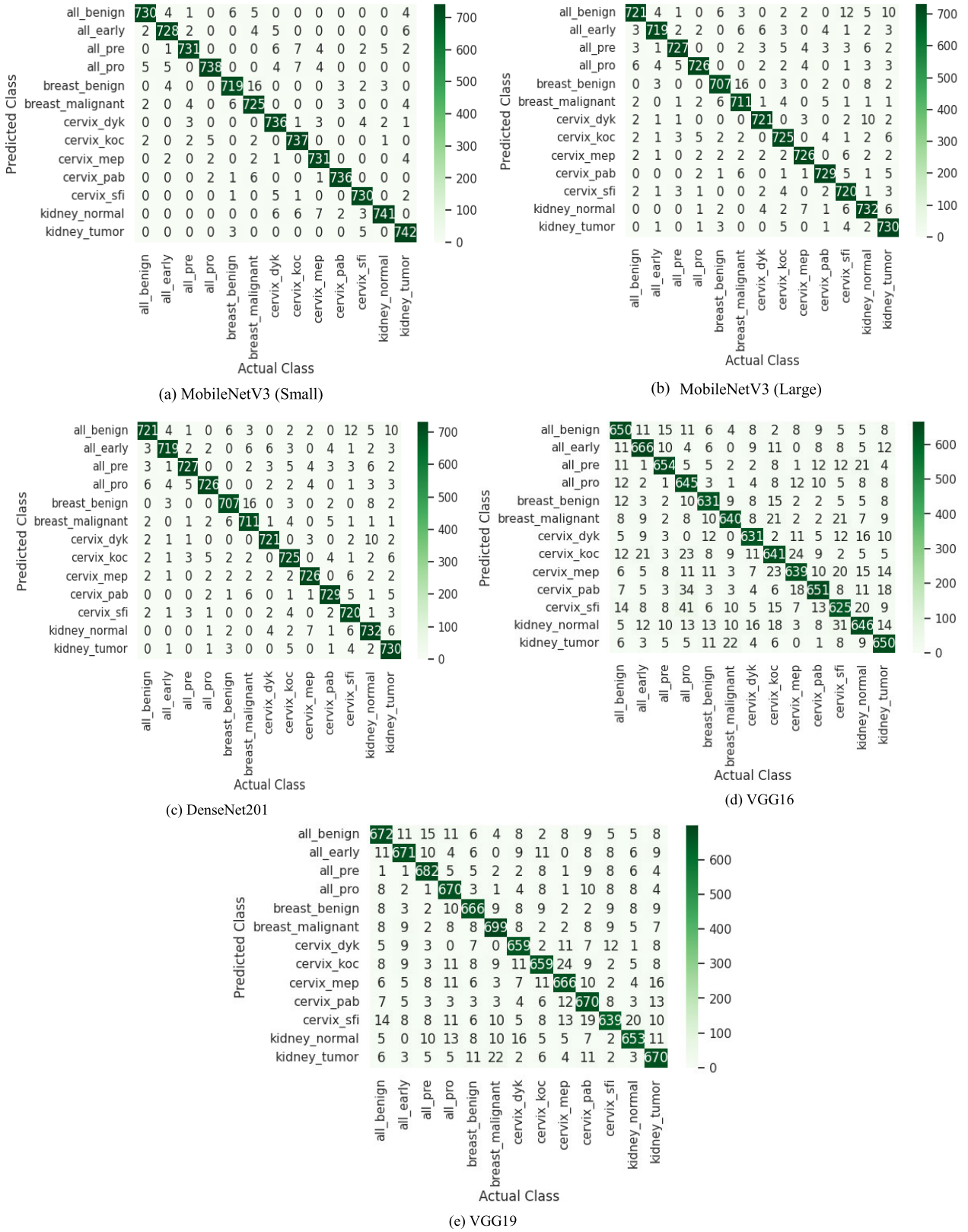

FIGURE 6. Confusion matrices for task set 1.

TABLE 4. Hyperparameters with their search space and fine-tuned values.

Parameter	Search Space	VGG16	VGG19	DenseNet201	MobileNetV3 Small	MobileNetV3 Large
Optimizer	RMSProp, Adagrad, ADAM, Stochastic GD, Nadam, Mini-Batch GD	ADAM	RMS Prop	ADAM	ADAM	SGD
Learning rate	1e-2, 1e-3, 1e-4, 1e-5, 1e-6	1e-4	1e-3	1e-3	1e-4	1e-2
Activation function	Relu, Elu, LeakyRelu, Parametric Leaky ReLU, Exponential LU, and Tanh	ReLU	LeakyReLU	Tanh	ReLU	ReLU
Number of neurons	32,64,128, 256, 512,1024	128	64	128	256	257
Number of epochs	50,75,100,125,150	100	125	150	100	100
Batch Size	16,32,64,128,256	32	32	128	128	128

TABLE 5. Overall performance of the proposed models.

VGG16		VGG19		DenseNet201		MobileNetV3 (Small)		MobileNetV3 (Large)	
Validation Accuracy (%)	Testing Accuracy (%)	Validation Accuracy (%)	Testing Accuracy (%)	Validation Accuracy (%)	Testing Accuracy (%)	Validation Accuracy (%)	Testing Accuracy (%)	Validation Accuracy (%)	Testing Accuracy (%)
79.61	75.82	80.93	76.34	84.78	79.82	86.51	84.52	83.04	81.67

these metrics, we have used the indices such as True Positive (TP), True Negative (TN), False Positive (FP), and False Negative (FN) (1, 2). We use Eq. (1) to Eq. (4) to calculate TP, FP, TP, and TN.

$$tp_i = c_{ii} \tag{1}$$

$$fp_i = \sum_{l=1}^{n} c_{li} - tp_i \tag{2}$$

$$fn_i = \sum_{l=1}^{n} c_{il} - tp_i \tag{3}$$

$$tn_i = \sum_{l=1}^{n} \sum_{k=1}^{n} c_{lk} - tp_i - fp_i - fn_i \tag{4}$$

$$\text{Accuracy} = (TP + TN)/(TP + TN + FP + FN) \tag{5}$$

$$\text{Recall} = TP/(TP + FN) \tag{6}$$

$$\text{Precision} = TP/(TP + FP) \tag{7}$$

$$F1\text{score} = \frac{(2 * \text{precision} * \text{recall})}{(\text{precision} + \text{recall})} \tag{8}$$

V. EXPERIMENTAL RESULTS AND FINDINGS

In this section, we present the performance of the proposed models on both old and new tasks without and with LwF.

A. RESULTS OF PROPOSED MODELS FOR TASK SET 1

We checked out how well the CNN models that were suggested worked. Experiments have been carried out using the tuned hyperparameters shown in Table 4, which produced the best results when the model was put through its training phase. Table 5 shows how well each model works for validation and test datasets. The class-wise performance of the developed models is presented in Table 6. We used the indices TP, FP, TN, and FN to find the values of several performance metrics, such as Accuracy, Precision, Recall, and F1-score. A supervised learning tool, the confusion matrix, compares predicted classes to actual classes. Figure 6 shows the confusion matrix for every model that has been developed.

The diagonals of the confusion matrix show the correct classifications. The actual classes are shown on the X-axis, while the predicted classes are shown on the Y-axis. In Fig 6(a), for instance, it is evident that MobileNetV3 (Small) incorrectly identified 5 all_benign as all_pro.

B. RESULTS OF PROPOSED MODELS FOR TASK SET 2

To demonstrate the power of LwF, we have also run the proposed models on task set 2, which consists of a dataset having 13 unseen classes belonging to the types of cancer which have not been included in task set 1. The results of this trial are shown in Table 7.

When testing task set 2 on the developed models, we obtained the results in Table 7. Since the models have been trained on task set 1, they gave good results for the test data set belonging to the task set 1. The features of the task set 2 are different from those of task set 1, and the models have learned the values for the task-specific parameters of task set 1. So, they could not perform well on the task set 2. To improve the performance of the models on the task set 2, we have trained the models using LwF and evaluated the performance. Figure 7 depicts the confusion matrices that indicate the performance of the models for task set 2 without LwF.

TABLE 6. Class wise performance of the proposed models.

Classifiers	Cancer Types	Class Labels	Accuracy (%)	Precision (%)	Recall (%)	F1score (%)
MobileNetV3 - Small	ALL	all_benign	84.52	97.33	98.52	97.92
		all_early		97.46	97.85	97.65
		all_pre		96.44	98.38	97.40
		all_pro		96.72	98.80	97.75
	Breast caner	breast_benign		96.25	97.69	96.97
		breast_malignant		97.45	95.39	96.41
	Cervical cancer	cervix_dyk		98.13	96.46	97.29
		cervix_koc		98.40	97.10	97.75
		cervix_mep		98.52	97.47	97.99
		cervix_pab		98.66	98.92	98.79
		cervix_sfi		98.78	97.86	98.32
	Kidney Cancer	kidney_normal		96.86	98.54	97.69
		kidney_tumor		98.93	96.99	97.95
	Macro Average			97.69	97.69	97.68
	Weighted Average			97.42	97.43	97.42
MobileNetV3 - Large	Acute lymphoblastic leukemia	all_benign	81.67	94.13	97.04	95.56
		all_early		95.74	97.69	96.70
		all_pre		95.78	97.85	96.80
		all_pro		96.03	97.84	96.93
	Breast cancer	breast_benign		95.41	96.98	96.19
		breast_malignant		96.73	95.05	95.89
	Cervical cancer	cervix_dyk		97.17	97.30	97.24
		cervix_koc		96.28	95.65	95.96
		cervix_mep		96.93	97.19	97.06
		cervix_pab		97.07	97.07	97.07
		cervix_sfi		97.43	94.49	95.94
	Kidney Cancer	kidney_normal		96.19	94.45	95.31
		kidney_tumor		97.72	94.19	95.93
	Macro Average			96.36	96.37	96.35
	Weighted Average			96.13	96.16	96.14
DenseNet201	Acute lymphoblastic leukemia	all_benign	79.82	87.53	93.10	90.23
		all_early		90.78	91.02	90.90
		all_pre		88.61	94.72	91.56
		all_pro		91.87	92.98	92.42
	Breast cancer	breast_benign		91.03	93.15	92.08
		breast_malignant		92.71	89.73	91.19
	Cervical cancer	cervix_dyk		94.34	91.03	92.65
		cervix_koc		93.41	93.28	93.34
		cervix_mep		95.72	94.51	95.11
		cervix_pab		94.06	94.44	94.25
		cervix_sfi		95.69	89.71	92.61
	Kidney Cancer	kidney_normal		93.73	94.49	94.11
		kidney_tumor		94.73	91.51	93.09
	Macro Average			92.63	92.59	92.58
	Weighted Average			92.27	92.31	92.26
VGG19	Acute lymphoblastic leukemia	all_benign		87.96	88.54	88.25
		all_early		89.11	91.17	90.13
		all_pre		92.92	90.69	91.79
		all_pro		92.03	87.93	89.93
	Breast cancer	breast_benign		89.4	89.64	89.52
		breast_malignant		90.19	90.54	90.37
	Cervical cancer	cervix_dyk		91.02	88.69	89.84

TABLE 6. *(Continued.)* **Class wise performance of the proposed models.**

		cervix_koc	76.34	86.03	89.42	87.69
		cervix_mep		88.21	88.92	88.56
		cervix_pab		90.54	86.01	88.22
		cervix_sfi		82.88	89.5	86.06
	Kidney Cancer	kidney_normal		87.65	89.82	88.72
		kidney_tumor		89.33	86.23	87.75
	Macro Average			89.02	89.01	88.99
	Weighted Average			89.22	89.25	89.21
VGG16	Acute lymphoblastic leukemia	all_benign		87.6	85.64	86.61
		all_early		88.8	88.21	88.5
		all_pre		88.62	90.33	89.47
		all_pro		89.71	79.63	84.37
	Breast cancer	breast_benign		88.62	87.03	87.82
		breast_malignant		85.68	89.76	87.67
	Cervical cancer	cervix_dyk		88.13	88.01	88.07
		cervix_koc	75.82	82.92	82.6	82.76
		cervix_mep		82.77	87.9	85.26
		cervix_pab		84.44	87.97	86.17
		cervix_sfi		80.03	82.02	81.01
	Kidney Cancer	kidney_normal		80.85	83.57	82.19
		kidney_tumor		89.04	84.53	86.72
	Macro Average			85.94	85.94	85.89
	Weighted Average			85.69	85.77	85.68

C. TRANSFER LEARNING USING LwF ON TASK SET 2

In this section, we show how the LwF compares to proposed models on task set 2 of CT/MRI images having symptoms of four different types of cancer, namely brain cancer, lung/colon, cervical and oral cancer. LwF utilizes only images from task set 2 to train the network but retains the model's original capabilities. When integrating LwF with the proposed models, the shared parameters (PS) of the feature extraction layers and the task-specific parameters (PO) of the classification layers for the task set 1, which was used for training, were maintained; however, the task-specific parameters (PB) of the new set of images from the task set 2 were modified. These models learned parameters that are effective on both task sets. We used CT/MRI images from the task set 2 for LwF training and retrained the network without task set 1. We added neurons to the output layer and randomly initialized the weights to retrain the models on the new images. The number of newly added parameters is, therefore, equal to the number of neurons added to the output layer multiplied by the number of neurons in the previously shared layer. This is a relatively modest number compared to the total network parameters. Reference [33] explains the training procedure. The values for accuracy, precision, recall, and F1-score for different models with LwF on CT/MRI images of the task set 2 are shown in Table 7, and Figure 8 shows the confusion matrices for these models.

VI. FINDINGS AND DISCUSSION

The objective of this study is to detect the presence of eight types of cancer using CT/MRI images. For this, we developed five models using pre-trained CNN architecture. The experimental results have been provided earlier in this section. Below, we discuss the results of our investigation.

In this study, several indicators have been employed to determine the efficacy of the transfer learning techniques: first, it is determined whether the proposed models could classify CT /MRI images using the transferred knowledge with fine-tuning. Since the weights of pre-trained models were used as-is during feature extraction, the resulting models may be less accurate. A few top layers' weights have been retrained during fine-tuning. This allows the models to gain image-specific characteristics and enhances their accuracy.

The performance of the developed models on the task set 1 is shown in Table 5. Among all the proposed models, the MobileNetV3 (small) exhibited the best performance on this task set. But, while using LwF, MobileNetV3 (large) has outperformed the other models. This is because this model uses a technique known as depth-wise separable convolution, which streamlines the learning process and boosts overall performance. Further, using an appropriate TPU hardware accelerator, this model could improve accuracy while simultaneously reducing the runtime and power consumption.

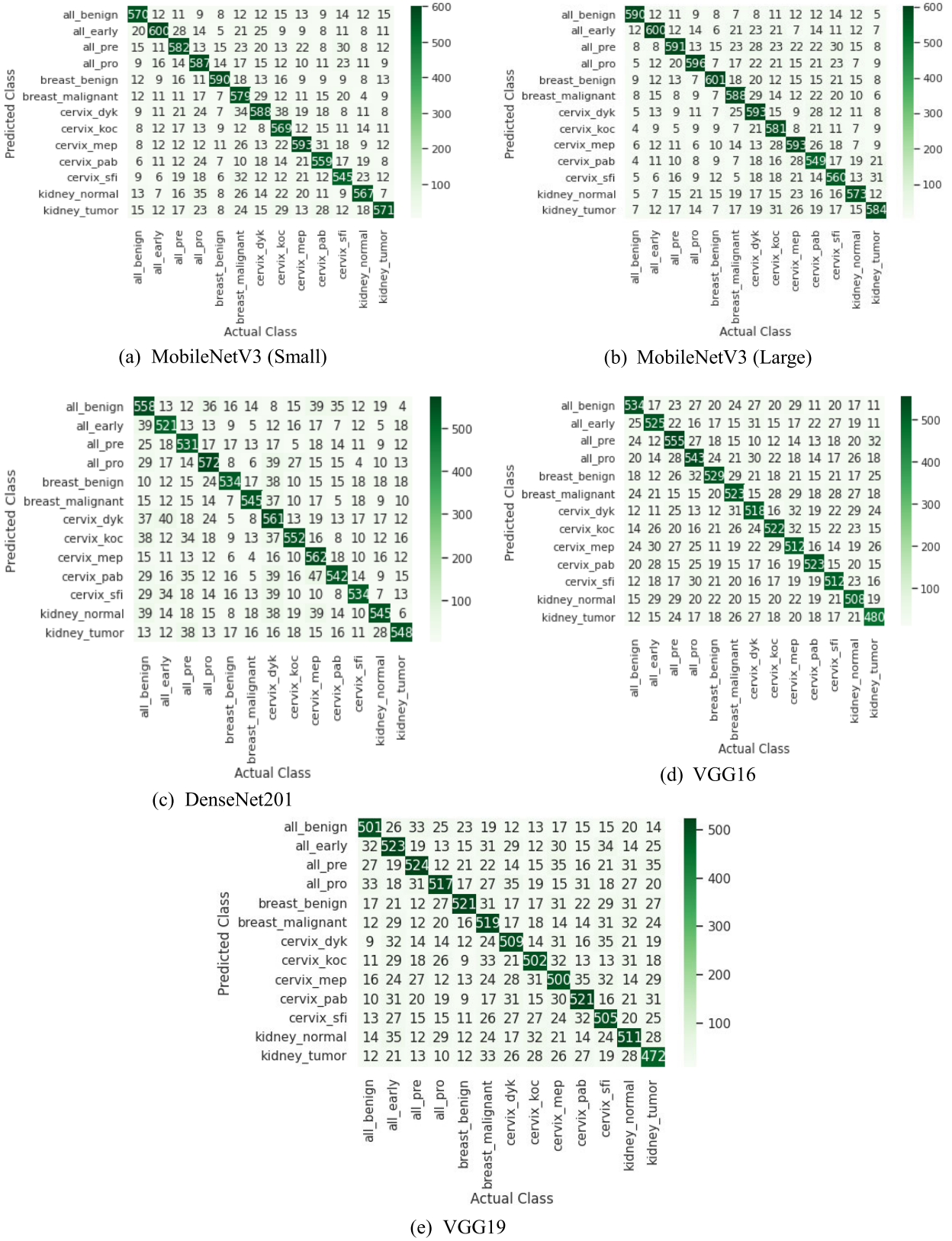

(a) MobileNetV3 (Small)

(b) MobileNetV3 (Large)

(c) DenseNet201

(d) VGG16

(e) VGG19

FIGURE 7. Confusion matrices for task set 2 (Without LwF).

TABLE 7. Performance of the proposed models task set 2.

Classifiers	Cancer Types	Class Labels	Accuracy (%)	Precision (%)	Recall (%)	F1score (%)
MobileNetV3 - Small	Brain cancer	brain_glioma	72.92	80.06	80.74	80.39
		brain_menin		78.02	82.19	80.05
		brain_tumor		75.39	75	75.19
	Lung/Colon Cancer	colon_aca		78.48	73.38	75.84
		colon_bnt		80.49	84.89	82.63
		lung_aca		78.56	69.42	73.71
		lung_bnt		73.87	75.19	74.52
		lung_scc		80.03	72.67	76.17
	Lymphoma	lymph_cll		76.12	76.71	76.42
		lymph_fl		77	76.16	76.58
		lymph_mcl		74.97	74.97	74.97
	Oral Cancer	oral_normal		75.1	79.63	77.3
		oral_scc		72.74	81.81	77.01
	Macro Average			76.99	77.14	76.98
	Weighted Average			76.71	76.93	76.74
MobileNetV3 - Large	Brain cancer	brain_glioma	74.05	82.98	88.32	85.57
		brain_menin		78.95	82.3	80.59
		brain_tumor		73.33	80.08	76.55
	Lung/Colon Cancer	colon_aca		76.9	82.09	79.41
		colon_bnt		78.46	84.29	81.27
		lung_aca		78.61	76.56	77.57
		lung_bnt		79.49	71.53	75.3
		lung_scc		82.88	72.08	77.11
	Lymphoma	lymph_cll		78.75	74.97	76.81
		lymph_fl		76.57	70.47	73.4
		lymph_mcl		76.92	72.73	74.77
	Oral Cancer	oral_normal		75.99	80.03	77.96
		oral_scc		74.39	81.45	77.76
	Macro Average			78.02	78.22	78.01
	Weighted Average			77.74	78.09	77.8
DenseNet201	Brain cancer	brain_glioma	68.52	71.45	63.7	67.35
		brain_menin		75.84	71.17	73.43
		brain_tumor		75.11	68.6	71.71
	Lung/Colon Cancer	colon_aca		74.38	72.96	73.66
		colon_bnt		71.77	79.94	75.64
		lung_aca		76.33	80.5	78.36
		lung_bnt		71.56	62.54	66.75
		lung_scc		71.23	76.56	73.8
	Lymphoma	lymph_cll		79.72	67.79	73.27
		lymph_fl		68.18	76.34	72.03
		lymph_mcl		71.68	78.41	74.89
	Oral Cancer	oral_normal		69.6	77.41	73.3
		oral_scc		72.01	78.62	75.17
	Macro Average			72.99	73.43	73.03
	Weighted Average			72.6	73.13	72.68
VGG19	Brain cancer	brain_glioma	64.72	68.46	70.82	69.62
		brain_menin		68.9	69.26	69.08
		brain_tumor		72.08	67.19	69.55
	Lung/Colon Cancer	colon_aca		68.3	67.37	67.83
		colon_bnt		67.47	70.35	68.88
		lung_aca		66.97	66.71	66.84
		lung_bnt		67.8	67.01	67.4
		lung_scc		67.27	69.32	68.28
	Lymphoma	lymph_cll		66.15	65.31	65.73

TABLE 7. *(Continued.)* **Performance of the proposed models task set 2.**

VGG16		lymph_fl	70.01	72.44	71.2
	Oral Cancer	lymph_mcl	69.19	67.9	68.54
		oral_normal	66.93	66.06	66.49
		oral_scc	67.32	67.61	67.46
	Macro Average		68.22	68.26	68.22
	Weighted Average		69.45	69.49	69.46
	Brain cancer	brain_glioma	68.35	70.86	69.58
		brain_menin	66.04	62.63	64.29
		brain_tumor	66.16	69.87	67.96
	Lung/Colon Cancer	colon_aca	63.99	69.96	66.84
		colon_bnt	64.88	75.4	69.75
		lung_aca	68.47	62.53	65.37
		lung_bnt	67.87	65.01	66.41
		lung_scc	66.4	67.56	66.98
	Lymphoma	lymph_cll	63.69	62.03	62.85
		lymph_fl	67.57	67.57	67.57
		lymph_mcl	65.84	63.76	64.79
	Oral Cancer	oral_normal	66.11	63.8	64.93
		oral_scc	64.92	61.54	63.19
	Macro Average		66.18	66.35	66.19
	Weighted Average		67.91	68.16	67.96

Due to the varied architectural design, such as the number of layers and convolution blocks, the models used in this work exhibited varied performance. MobileNet is a lightweight deep neural network with better classification accuracy and fewer parameters. Dense blocks from DenseNets are used into MobileNet to further minimize the amount of network parameters and increase classification accuracy. Despite being 32 times smaller than VGG16, MobileNet has higher accuracy and is more effective at gathering knowledge.

When we tested how well the proposed models could transfer knowledge over a new task set 2 CT/MRI images having symptoms of four different types of cancer, we found that the models were not very accurate. This is because the models have yet to be retrained on task set 2. After retraining the model using task set 2, we tested the models again with task set 1 and found that they were less accurate than before. As the number of tasks increases, storing and retraining such images becomes impossible. Adding new capabilities to a CNN wipes out the training data for the existing capabilities. So, we turned to LwF, which retrains the network using task set 2 while keeping the network's original abilities. Table 8 shows that LwF does better than most fine-tuning techniques on the task set 2 images. In Table 9, we can see how the models with fine-tuning and LwF compare to each other.

For increased performance on the task set 2, LwF may be an alternative to fine-tuning. Subsequently, the accuracy of the task set 1 will be equivalent to that of the original models provided the models are maintained in such a way that task-specific characteristics of task set 1 give identical outputs on all relevant images. To summarize, in this study, we implemented LwF, a multi-task learning strategy for CNNs that enables CNNs to acquire good performance on new tasks while maintaining performance on previous tasks. As a result of this work, we understood how LwF could be utilized in situations where the initial training dataset is unavailable. On a new dataset, the efficacy of LwF has been validated, and experimental findings demonstrated that it outperforms fine-tuning. According to the experimental findings, contemporary models like MobileNet, DenseNet, etc. perform significantly better than traditional models like VGGNet, AlexNet, etc.

A. BLACK BOX ISSUES

Deep learning model integration in cancer care could increase the precision and speed of diagnosis, support clinical decision-making, and result in better health outcomes. These models, however, are regarded as ''black box'' models. Black boxes are frequently employed in the healthcare sector to analyze huge amounts of data and make predictions based on that data, but patients and healthcare professionals may find the lack of openness about how such decisions are made to be concerning. A black box's predictions or decisions could not be clear to patients or healthcare professionals, which might breed mistrust or muddled thinking. But by expanding such a black box, explainable AI can be produced. If people can understand how an AI system arrived at its choice, the system is considered to be explainable. This would make it easier to gain research information in healthcare.

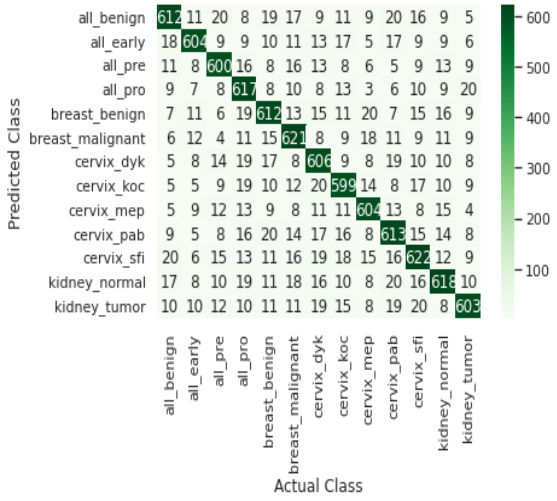

(a) MobileNetV3 (Small)

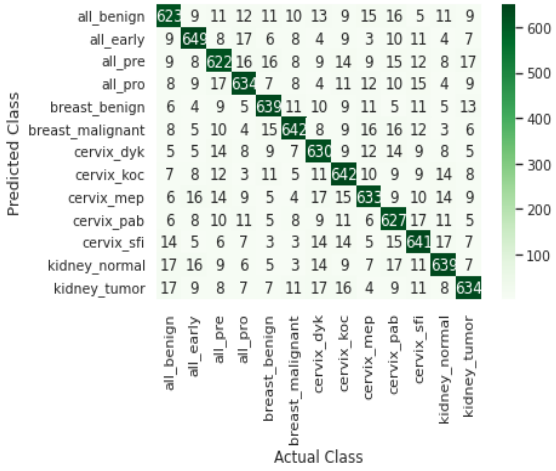

(b) MobileNetV3 (Large)

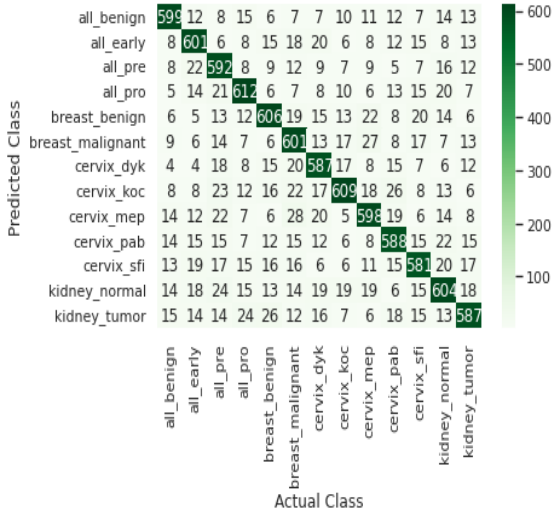

(c) DenseNet201

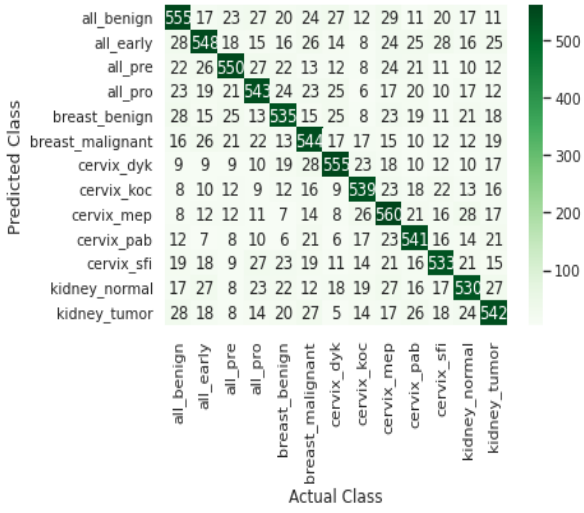

(d) VGG16

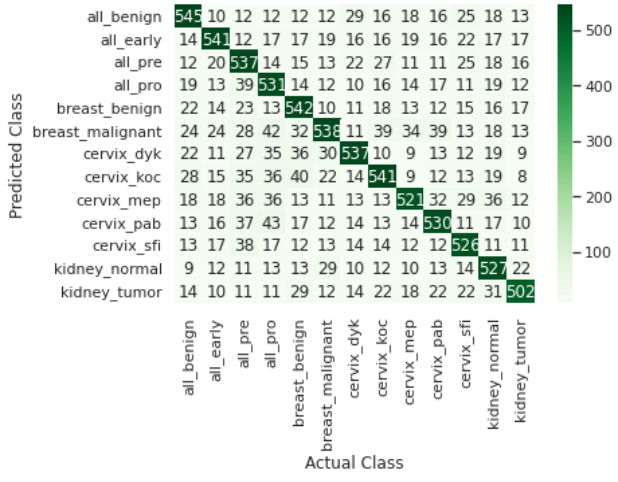

(e) VGG19

FIGURE 8. **Confusion matrices for the task set 2 (With LwF).**

TABLE 8. Performance of the proposed models with LWF on task set 2.

Classifiers	Cancer Types	Class Labels	Accuracy (%)	Precision (%)	Recall (%)	F1score (%)
MobileNetV3 - Small	Brain cancer	brain_glioma	78.21	79.9	83.38	81.6
		brain_menin		81.95	85.8	83.83
		brain_tumor		83.1	82.53	82.82
	Lung/Colon Cancer	colon_aca		84.75	78.2	81.34
		colon_bnt		80.42	80.42	80.42
		lung_aca		83.47	80.13	81.76
		lung_bnt		81.78	78.29	80
		lung_scc		81.28	80.19	80.73
	Cervical cancer	lymph_cll		83.66	83.2	83.43
		lymph_fl		80.34	79.2	79.77
		lymph_mcl		78.54	80.15	79.34
	Oral Cancer	oral_normal		79.13	81.96	80.52
		oral_scc		79.76	85.05	82.32
	Macro Average			81.39	81.42	81.37
	Weighted Average			81.43	81.51	81.44
MobileNetV3 - Large	Brain cancer	brain_glioma	79.95	82.63	84.76	83.68
		brain_menin		87.11	86.42	86.76
		brain_tumor		81.52	82.93	82.22
	Lung/Colon Cancer	colon_aca		84.76	85.79	85.27
		colon_bnt		86.59	86.47	86.53
		lung_aca		85.15	88.19	86.64
		lung_bnt		85.71	82.89	84.28
		lung_scc		85.71	82.63	84.14
	Cervical cancer	lymph_cll		83.18	85.2	84.18
		lymph_fl		85.42	81.22	83.27
		lymph_mcl		85.35	82.82	84.07
	Oral Cancer	oral_normal		84.08	85.66	84.86
		oral_scc		83.64	86.14	84.87
	Macro Average			84.68	84.7	84.67
	Weighted Average			84.59	84.63	84.59
DenseNet201	Brain cancer	brain_glioma	77.84	83.08	83.54	83.31
		brain_menin		81.44	80.13	80.78
		brain_tumor		82.68	75.22	78.78
	Lung/Colon Cancer	colon_aca		82.26	81.6	81.93
		colon_bnt		79.84	80.59	80.21
		lung_aca		80.67	75.98	78.26
		lung_bnt		81.41	78.37	79.86
		lung_scc		77.48	83.2	80.24
	Cervical cancer	lymph_cll		78.79	79.63	79.21
		lymph_fl		79.03	78.93	78.98
		lymph_mcl		77.26	79.81	78.51
	Oral Cancer	oral_normal		75.69	78.34	76.99
		oral_scc		76.53	80.74	78.58
	Macro Average			79.71	79.7	79.66
	Weighted Average			79.28	79.35	79.28
VGG19	Brain cancer	brain_glioma	70.12	69.99	71.8	70.88
		brain_menin		69.28	72.87	71.03
		brain_tumor		72.56	75.97	74.22
	Lung/Colon Cancer	colon_aca		71.45	72.3	71.87
		colon_bnt		70.77	72.4	71.57
		lung_aca		73.12	69.57	71.3
		lung_bnt		76.13	75.82	75.98
		lung_scc		76.24	75.81	76.02

TABLE 7. *(Continued.)* **Performance of the proposed models with LWF on task set 2.**

VGG16	Cervical cancer	lymph_cll	65.91	75.68	68.21	71.75
		lymph_fl		77.07	71.75	74.31
		lymph_mcl		71.45	73.42	72.42
	Oral Cancer	oral_normal		69.46	72.31	70.86
		oral_scc		71.22	72.07	71.65
	Macro Average			72.65	72.64	72.6
	Weighted Average			72.44	72.5	72.43
	Brain cancer	brain_glioma		73.85	72.38	73.11
		brain_menin		72.81	75.03	73.91
		brain_tumor		72.47	63.48	67.67
	Lung/Colon Cancer	colon_aca		73.04	64.76	68.65
		colon_bnt		74.66	68.43	71.41
		lung_aca		62.92	73.4	67.76
		lung_bnt		69.74	75.1	72.32
		lung_scc		68.31	71.47	69.85
	Cervical cancer	lymph_cll		66.12	74.22	69.93
		lymph_fl		70.95	71.14	71.05
		lymph_mcl		74.08	71.27	72.65
	Oral Cancer	oral_normal		75.83	68.8	72.14
		oral_scc		69.92	75.83	72.75
	Macro Average			71.13	71.18	71.02
	Weighted Average			71.07	71.35	71.07

TABLE 8. **Performance of the models on task set 2 with and without LWF.**

Approach	Testing Accuracy (%)				
	VGG16	VGG19	DenseNet201	MobileNetV3 (Small)	MobileNetV3 (Large)
Fine-tuned (Without LwF)	62.56	64.72	68.52	72.92	74.05
LwF	65.91	70.12	77.84	78.21	79.95

TABLE 9. **LwF vs fine tuned models.**

Task set	Performance of the Models	
	Fine-tuned	LwF
Task set 1	Good	Good
Task set 2	Moderate	Good
Need for task set 1 to increase the accuracy	Yes	No

VII. CONCLUSION

Cancer causes one in six deaths worldwide. Therefore, cancer diagnostic and treatment techniques have received much investigation. In this attempt, we presented improved CNN variants for detecting multiple types of cancer. Transfer learning has been utilized in this study since it does not require vast datasets and retrains a few top layers while using little processing effort. In addition, Bayesian optimization is utilized to choose the most appropriate values for the hyperparameters employed throughout the training process. Further, we split the images into two task sets, one for fine-tuning the models and another to verify the multitasking ability of the developed models. Finally, LwF, a multitask learning method, has been employed to inculcate multitasking ability into the developed models. The results demonstrate that LwF maintained the knowledge learned from task set 1 and performed better than fine-tuned models on the task set 2. From this study, we understood that LwF could be used where the original training dataset is unavailable. Of all models, we found that MobileNetV3 outperformed with a substantial performance improvement.

To further extend this work, we plan to include more types of cancer in our task sets and calibrate multitask learning with extensive experiments. We will also investigate other types of imaging techniques that aid in the detection of cancer cells.

REFERENCES

[1] *Top Opportunities for Artificial Intelligence to Improve Cancer Care*. Accessed: Nov. 29, 2021. [Online]. Available: https://healthitanalytics.com/features/top-opportunities-for-artificial-intelligence-to-improve-cancer-care

[2] M. Subramanian, K. Shanmugavadivel, and P. S. Nandhini, "On fine-tuning deep learning models using transfer learning and hyper-parameters optimization for disease identification in maize leaves," *Neural Comput. Appl.*, vol. 34, no. 16, pp. 13951–13968, Aug. 2022.

[3] M. Subramanian, "Hyperparameter optimization for transfer learning of VGG16 for disease identification in corn leaves using Bayesian optimization," *Big Data*, vol. 10, no. 3, pp. 215–229, Jun. 2022.

[4] S. Krishnamoorthy, A. Shanthini, G. Manogaran, V. Saravanan, A. Manickam, and R. D. J. Samuel, "Regression model-based feature filtering for improving hemorrhage detection accuracy in diabetic retinopathy treatment," *Int. J. Uncertainty, Fuzziness Knowl.-Based Syst.*, vol. 29, no. 1, pp. 51–71, Apr. 2021.
[5] S. Roy, T. Meena, and S.-J. Lim, "Demystifying supervised learning in healthcare 4.0: A new reality of transforming diagnostic medicine," *Diagnostics*, vol. 12, no. 10, p. 2549, Oct. 2022.
[6] S. Krishnamoorthy, Y. Zhang, S. Kadry, and W. Yu, "Framework to segment and evaluate multiple sclerosis lesion in MRI slices using VGG-UNet," *Comput. Intell. Neurosci.*, vol. 2022, pp. 1–10, Jun. 2022.
[7] S. Rezayi, N. Mohammadzadeh, H. Bouraghi, S. Saeedi, and A. Mohammadpour, "Timely diagnosis of acute lymphoblastic leukemia using artificial intelligence-oriented deep learning methods," *Comput. Intell. Neurosci.*, vol. 2021, pp. 1–12, Nov. 2021.
[8] S. R. Gunasekara, H. N. T. K. Kaldera, and M. B. Dissanayake, "A systematic approach for MRI brain tumor localization and segmentation using deep learning and active contouring," *J. Healthcare Eng.*, vol. 2021, pp. 1–13, Feb. 2021.
[9] V. K. Reshma, N. Arya, S. S. Ahmad, I. Wattar, S. Mekala, S. Joshi, and D. Krah, "Detection of breast cancer using histopathological image classification dataset with deep learning techniques," *BioMed Res. Int.*, vol. 2022, pp. 1–13, Mar. 2022.
[10] S. Zhao, Y. He, J. Qin, and Z. Wang, "A semi-supervised deep learning method for cervical cell classification," *Anal. Cellular Pathol.*, vol. 2022, pp. 1–12, Feb. 2022.
[11] M. Pedersen, M. B. Andersen, H. Christiansen, and N. H. Azawi, "Classification of renal tumour using convolutional neural networks to detect oncocytoma," *Eur. J. Radiol.*, vol. 133, Dec. 2020, Art. no. 109343.
[12] M. Masud, N. Sikder, A.-A. Nahid, A. K. Bairagi, and M. A. AlZain, "A machine learning approach to diagnosing lung and colon cancer using a deep learning-based classification framework," *Sensors*, vol. 21, no. 3, p. 748, Jan. 2021.
[13] A. H. Khan, S. Abbas, M. A. Khan, U. Farooq, W. A. Khan, S. Y. Siddiqui, and A. Ahmad, "Intelligent model for brain tumor identification using deep learning," *Appl. Comput. Intell. Soft Comput.*, vol. 2022, pp. 1–10, Jan. 2022.
[14] S. A. Alanazi, M. M. Kamruzzaman, M. N. I. Sarker, M. Alruwaili, Y. Alhwaiti, N. Alshammari, and M. H. Siddiqi, "Boosting breast cancer detection using convolutional neural network," *J. Healthcare Eng.*, vol. 2021, pp. 1–11, Apr. 2021.
[15] A. Akilandeswari, D. Sungeetha, C. Joseph, K. Thaiyalnayaki, K. Baskaran, R. J. Ramalingam, H. Al-Lohedan, D. M. Al-dhayan, M. Karnan, and K. M. Hadish, "Automatic detection and segmentation of colorectal cancer with deep residual convolutional neural network," *Evidence-Based Complementary Alternative Med.*, vol. 2022, pp. 1–8, Mar. 2022.
[16] K. Warin, W. Limprasert, S. Suebnukarn, S. Jinaporntham, and P. Jantana, "Automatic classification and detection of oral cancer in photographic images using deep learning algorithms," *J. Oral Pathol. Med.*, vol. 50, no. 9, pp. 911–918, Oct. 2021.
[17] A. B. Tufail, Y.-K. Ma, M. K. A. Kaabar, F. Martínez, A. R. Junejo, I. Ullah, and R. Khan, "Deep learning in cancer diagnosis and prognosis prediction: A minireview on challenges, recent trends, and future directions," *Comput. Math. Methods Med.*, vol. 2021, pp. 1–28, Oct. 2021.
[18] *Acute Lymphoblastic Leukemia (ALL) Image Dataset*. Kaggle, San Francisco, CA, USA, 2021.
[19] F. Spanhol. *Breast Cancer Histopathological Database*. Accessed: Nov. 30, 2022. [Online]. Available: https://www.kaggle.com/datasets/anaselmasry/breast-cancer-dataset
[20] Sipakmed. *A New Dataset for Feature and Image Based Classification of Normal and Pathological Cervical Cells in Pap Smear Images*. Accessed: Oct. 2018. [Online]. Available: https://www.kaggle.com/datasets/prahladmehandiratta/cervical-cancer-largest-dataset-sipakmed
[21] *CT Kidney Dataset: Normal-Cyst-Tumor and Stone*. Accessed: Dec. 2021. [Online]. Available: https://www.kaggle.com/datasets/nazmul0087/ct-kidney-dataset-normal-cyst-tumor-and-stone
[22] A. A. Borkowski, L. B. Thomas, C. P. Wilson, L. A. DeLand, and S. M. Mastorides. *Lung and Colon Cancer Histopathological Image Dataset (LC25000)*. Accessed: Dec. 2019. [Online]. Available: https://www.kaggle.com/datasets/andrewmvd/lung-and-colon-cancer-histopathological-images
[23] N. V. Orlov, W. W. Chen, D. M. Eckley, T. J. Macura, L. Shamir, and E. S. Jaffe, "Automatic classification of lymphoma images with transform-based global features," *IEEE Trans. Inf. Technol. Biomed.*, vol. 14, no. 4, pp. 1003–1013, Jul. 2010.
[24] *Histopathologic Oral Cancer Detection Using CNNs*. Accessed: Dec. 2020. [Online]. Available: https://www.kaggle.com/datasets/ashenafifasilkebede/dataset
[25] J. Cheng, "Brain tumor dataset," Figshare. Accessed: Apr. 2017, doi: 10.6084/m9.figshare.1512427.v5.
[26] O. S. Naren and M. Subramanian. (2022). *Multi Cancer Dataset*. [Online]. Available: https://www.kaggle.com/datasets/obulisainaren/multi-cancer
[27] Y. Bengio, I. Goodfellow, and A. Courville, "Deep learning," *Nature*, vol. 521, no. 7553, pp. 436–444, May 2016.
[28] Y. LeCun, F. J. Huang, and L. Bottou, "Learning methods for generic object recognition with invariance to pose and lighting," in *Proc. IEEE Comput. Soc. Conf. Comput. Vis. Pattern Recognit.*, Washington, DC, USA, Jul. 2004, p. 104.
[29] Y. LeCun, L. D. Jackel, L. Bottou, C. Cortes, J. S. Denker, and H. H. Drucker, "Learning algorithms for classification: A comparison on handwritten digit recognition," *Neural Netw., Stat. Mech. Perspective*, vol. 261, no. 276, pp. 261–276, 1995.
[30] M. Raghu, C. Zhang, J. Kleinberg, and S. Bengio, "Transfusion: Understanding transfer learning for medical imaging," in *Proc. Adv. Neural Inf. Process. Syst.*, 2019, pp. 3347–3357.
[31] A. Canziani, A. Paszke, and E. Culurciello, "An analysis of deep neural network models for practical applications," 2016, *arXiv:1605.07678*.
[32] J. Chen, J. Chen, D. Zhang, Y. Sun, and Y. A. Nanehkaran, "Using deep transfer learning for image-based plant disease identification," *Comput. Electron. Agricult.*, vol. 173, Jun. 2020, Art. no. 105393.
[33] Z. Li and D. Hoiem, "Learning without forgetting," *IEEE Trans. Pattern Anal. Mach. Intell.*, vol. 40, no. 12, pp. 2935–2947, Dec. 2018.
[34] *When Breast Cancer Metastasizes to the Brain?* Accessed:b Feb. 21, 2022. [Online]. Available: https://www.healthline.com/health/breast-cancer/breast-cancer-metastasis-to-brain#overview
[35] *Can Cervical Cancer Lead to Kidney Failure?* Accessed: Oct. 21, 2022. [Online]. Available: https://www.healthline.com/health/cervical-cancer/cervical-bcancer-and-kidney-failure
[36] J. P. Leone and B. A. Leone, "Breast cancer brain metastases: The last frontier," *Exp. Hematol. Oncol.*, vol. 4, no. 1, pp. 1–10, Dec. 2015.
[37] M. I. Sameen, B. Pradhan, and S. Lee, "Application of convolutional neural networks featuring Bayesian optimization for landslide susceptibility assessment," *Catena*, vol. 186, Mar. 2020, Art. no. 104249.
[38] U. Yunus, J. Amin, M. Sharif, M. Yasmin, S. Kadry, and S. Krishnamoorthy, "Recognition of knee osteoarthritis (KOA) using YOLOv2 and classification based on convolutional neural network," *Life*, vol. 12, no. 8, p. 1126, Jul. 2022.

MALLIGA SUBRAMANIAN received the Ph.D. degree from Anna University, Chennai, in 2010. She has more than 26 years of teaching experience. She has done consultancy project for BPL and offered several courses on the latest technology. She is working as a Professor with the Department of Computer Science and Engineering, Kongu Engineering College, Tamil Nadu, India. Currently, she is guiding four research scholars. She has also guided many U.G. and P.G. projects. She has published more than 50 articles in international journals and presented more than 60 papers in national and international conferences in her research and other technical areas. Her main research interests include network security, the IoT, deep learning, and NLP.

JAEHYUK CHO received the Ph.D. degree in computer science, focusing on mobile and embedded computing systems, from Chung-Ang University, South Korea, in 2011. He was a Professor at the Department of Electronic Engineering, Soongsil University. He was a National Research and Development Program Project Manager at the Korea Institute of S&T Evaluation and Planning (KISTEP), Seoul. He was a Senior Researcher at LG CNS, Seoul. He is currently a full-time Professor with the Department of Software Engineering, Jeonbuk National University, Jeonju, South Korea. His research interests include applied AI, data process, bigdata of sensors, the IoT, smart city, and SW platform systems.

VEERAPPAMPALAYAM EASWARAMOORTHY SATHISHKUMAR received the bachelor's degree in information technology from the Madras Institute of Technology, Anna University, in 2013, the master's degree in biometrics and cyber security from PSG College of Technology, in 2015, and the doctoral degree from Sunchon National University, in 2021. He worked as a Research Associate at VIT University, from 2015 to 2017. He was a Postdoctoral Researcher at the Department of Industrial Engineering, Hanyang University, Seoul, South Korea. In 2021, he worked as an Assistant Professor at the Department of Computer Science and Engineering, Kongu Engineering College. He is currently a Postdoctoral Researcher with the Department of Software Engineering, Jeonbuk National University, South Korea. He published more than 60 research papers in reputed journals and conferences. His research interests include data mining, big data analytics, cryptography, digital forensics, artificial intelligence, and computational chemistry. He received the South Korea's prestigious Global Korean Scholarship for pursuing the doctoral degree. He is a reviewer for more than 200 journals and has reviewed more than 2000 research articles. He is currently serving as an Academic Editor for the journals *PLOS ONE* and *Journal of Healthcare Engineering*.

OBULI SAI NAREN was studying at Kongu Engineering College, Department of Computer Science Engineering as an undergraduate and graduated with the bachelor's degree in 2022. He is a Project Engineer with Soliton Technologies, India.